

## Article

# Study of a New Photocatalytic Film Process Combined with a Constructed Wetland and an Analysis of Reoxygenation Pathways in a Water Body

Shihao Chen <sup>1,†</sup>, Ming Ye <sup>1,†</sup>, Nuo Chen <sup>1</sup>, Wenbin Pan <sup>1,\*</sup>  and Wenxin Dai <sup>2</sup>

<sup>1</sup> College of Environment & Safety Engineering, Fuzhou University, Fuzhou 350108, China; chenshihaochenjian@163.com (S.C.); 18305967871@163.com (M.Y.); chennuo20200226@163.com (N.C.)

<sup>2</sup> State Key Laboratory Breeding Base of Photocatalysis, Fuzhou University, Fuzhou 350002, China; daiwenxin@fzu.edu.cn

\* Correspondence: wenbinpan@fzu.edu.cn

† These authors contributed equally to this work.

**Abstract:** Pollution in water environments hinders both social progress and economic development. Wastewater treatment and the sustainable use of water resources are important factors in solving this problem. In a previous study, the authors proposed a process that used photocatalytic film as a back-end treatment in a composite iron–carbon constructed wetland ( $W_{IC}$ &PF) to restore a mildly eutrophic water body. This method has strong reoxygenation effects, and can efficiently remove pollutants; these are qualities that have not been mentioned in previous studies regarding constructed wetlands. In this study, the authors further investigated the effectiveness of this process by using a photocatalytic film as a front-end treatment for a composite iron–carbon constructed wetland (PF& $W_{IC}$ ) to restore a mildly eutrophic water body. The results showed  $NH_4^+$ –N, TN, TP, COD, and chlorophyll *a* removal rates using PF& $W_{IC}$  of  $79.1 \pm 6.6\%$ ,  $76.8 \pm 6.5\%$ ,  $77.0 \pm 5.4\%$ ,  $77.3 \pm 7.2\%$ , and  $91.7 \pm 5.6\%$ , respectively. The DO concentration of the water body increased compared with that of the effluent. The bacterial species and their abundance in the lake water also changed significantly, and photosynthetic autotrophic bacteria (*Cyanobium PCC-6307*) became the most dominant bacteria, and this played an important role in reoxygenating the water body. In comparing these results to those of our previous study, the removal of pollutants with PF& $W_{IC}$  was close to that with  $W_{IC}$ &PF, but the reoxygenation effect of PF& $W_{IC}$  on the water body was significantly worse than that of  $W_{IC}$ &PF; thus,  $W_{IC}$ &PF is the more reasonable choice for treating eutrophic water bodies.

**Keywords:** water pollution; sustainable utilization; constructed wetland; photocatalytic film; reoxygenation; photoautotrophic bacteria



**Citation:** Chen, S.; Ye, M.; Chen, N.; Pan, W.; Dai, W. Study of a New Photocatalytic Film Process Combined with a Constructed Wetland and an Analysis of Reoxygenation Pathways in a Water Body. *Sustainability* **2024**, *16*, 3123. <https://doi.org/10.3390/su16083123>

Academic Editor: Elena Cristina Rada

Received: 15 March 2024

Revised: 30 March 2024

Accepted: 2 April 2024

Published: 9 April 2024



**Copyright:** © 2024 by the authors. Licensee MDPI, Basel, Switzerland. This article is an open access article distributed under the terms and conditions of the Creative Commons Attribution (CC BY) license (<https://creativecommons.org/licenses/by/4.0/>).

## 1. Introduction

Pollution in water environments is one of the major problems faced by human society in regard to the process of development, and different countries and regions face this issue to different degrees [1,2]. Water environments can be polluted by the continuous accumulation of pollutants. These pollutants gradually exceed their water environments' capacity, and this leads to water quality deterioration, algae outbreaks, aquatic organism death, foul-smelling water bodies, eutrophication, and other phenomena [3–5]. These problems are a significant burden on economic and social development [6], and an increasing amount of technologies are being developed to treat the problem of water environment pollution. Wastewater treatment technologies should follow an effective and sustainable water management strategy [7]. Therefore, the development of safe wastewater treatment processes to promote water resource recycling and minimize pollutant discharge has become important to environmentally sustainable development. A constructed wetland refers to the interrelationship between the symbiotic system of plants and microorganisms and the

treatment environment, or medium, in the process of wastewater treatment, which purifies wastewater and promotes the cycling of nutrients such as carbon, nitrogen, and phosphorus in a highly efficient way via physical, chemical, and biological actions [8]. Constructed wetlands have multiple advantages, including the efficient removal of pollutants, reduced costs and energy consumption, ecological balance and biodiversity, enhanced landscape value, and water resource recycling. The comprehensive benefits of constructed wetlands are significant, so they have become one of the most commonly used water treatment technologies [9–11]. Ecological wastewater treatment technology provides a sustainable wastewater treatment process that combines wastewater treatment with water resource utilization, mainly via the purifying effects of natural ecosystems [12]. Constructed wetlands are a typical wastewater treatment process that can improve treatment efficiency by establishing a diverse ecological structure and regulation system for hydraulic load distribution [13]. Wastewater treatment is the only technology that can regenerate water resources, and constructed wetlands, as a fundamental economic resource, play a significant role in both water recycling and wastewater treatment processes [14].

Constructed wetlands mimic natural wetlands, purifying wastewater through an artificially designed structure that contains a substrate, aquatic plants, and microorganisms [15]. Depending on the engineering design and water flow pattern, constructed wetlands can be categorized into surface flow constructed wetlands (SFCW), horizontal subsurface flow constructed wetlands (HSSFCW), or vertical subsurface flow constructed wetlands (VSSFCW) [16–18]. Regardless of the type of constructed wetland used to treat wastewater, in general, without aeration, the dissolution of oxygen (DO) concentrations in wastewater is a decreasing process from the influent to the effluent, as DO must be consumed during the aerobic decomposition of microorganisms to degrade pollutants in water bodies [19]. Indeed, the aerobic decomposition of microorganisms is one of the main reasons why constructed wetlands are efficient in removing pollutants [20]. However, reducing DO concentrations is not conducive to restoring a water body's environment; a high concentration of DO in a water body will affect the survival of aquatic organisms, and a low concentration will cause most of the aquatic organisms to die of hypoxia [21–23], which will then destroy the aquatic biodiversity. The concentration of DO also affects the extent of chemical reactions in water. When the concentration of DO is high, the degradation of organic matter and  $\text{NH}_4^+ - \text{N}$  is favored [24,25]; when the concentration of DO is low, the denitrification of  $\text{NO}_3^- - \text{N}$  and  $\text{NO}_2^- - \text{N}$  is more complete [26,27]. In addition, DO is an important indicator of a water body's ability to self-purify. This self-purification ability depends on the length of time it takes for the DO in the water body to return to its initial state after being consumed. The shorter the time, the stronger the self-purification ability and the lighter the pollution; the longer the time, the weaker the self-purification ability and the heavier the pollution [28,29].

Iron and carbon fillers in wastewater treatment can achieve good results. Because of microelectrolysis, iron and carbon filler can form countless tiny primary batteries in which iron is the anode and carbon is the cathode; thus, the Fe will lose electrons, becoming  $\text{Fe}^{2+}$ . At the same time, the cathode and anode in the primary cell will react, forming a microelectric field in the wastewater; under the microelectric field's action, small colloidal particles and small molecular pollutants in the wastewater undergo electrophoresis, moving in the opposite direction of the charge and, ultimately, the electrode will aggregate large particles, resulting in flocculation and precipitation [30]. The Fe-C microelectrolysis reaction mechanism is as follows:

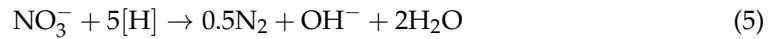
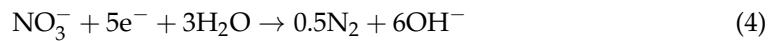
The reaction at the anode:



The reaction at the cathode:



The electrons generated by Equations (1) and (2) reduce  $\text{NO}_3^- - \text{N}$ , while  $\text{Fe}^{2+}$  and  $[\text{H}]$  from Equation (3) act as electron donors for denitrogenation in the following reaction:



$\text{Fe}^{2+}$  and  $\text{Fe}^{3+}$  form precipitates of  $\text{Fe}_3(\text{PO}_4)_2$  and  $\text{FePO}_4$  with  $\text{PO}_4^{3-}$  to remove phosphorus.  $\text{Fe}^{2+}$  and  $[\text{H}]$  have reducing properties that can not only reduce nitro in wastewater but also break down some organic macromolecules and decompose them into smaller molecules. Given the excellent mechanism of Fe-C microelectrolysis, a large number of scholars have investigated Fe-C filler as an artificial wetland substrate [31].

Photocatalytic denitrification and phosphorus removal are chemical processes that use a photocatalyst (e.g.,  $\text{TiO}_2$ ) activated under light conditions to generate electron ( $\text{e}^-$ ) and hole pairs by absorbing ultraviolet or visible light; this, in turn, generates free radicals such as hydroxyl radicals ( $\cdot\text{OH}$ ) with strong oxidizing abilities [32]. These free radicals can effectively decompose nitrogen and phosphorus compounds in water—such as  $\text{NH}_4^+ - \text{N}$ ,  $\text{NO}_3^- - \text{N}$ ,  $\text{NO}_2^- - \text{N}$ , inorganic phosphorus, organic phosphorus, etc.—and convert them into harmless or low-toxicity substances, thus removing nitrogen and phosphorus [33]. Thus, this process is important for treating nitrogen and phosphorus pollution in water bodies.

Therefore, the authors proposed a composite iron–carbon constructed wetland combined with photocatalytic film ( $\text{W}_{\text{IC}}\&\text{PF}$ ) to restore a mildly eutrophic water body from a previous study. Our results showed that using photocatalytic film for the back-end treatment of composite iron–carbon constructed wetlands not only ensures efficient pollutant removal efficiency but also effectively improves the reoxygenation effect of the constructed wetland; this is a quality that has not been mentioned in previous studies on constructed wetlands [34]. The present study was conducted at the same time as the previous study. We used photocatalytic film as a front-end treatment for the composite iron–carbon constructed wetland to more deeply explore its effects on the reoxygenation of a water body when it is not also affected by the aforementioned constructed wetland. This process was compared with the previous study to analyze the differences between photocatalytic film as a front-end or back-end treatment, as well as to find a better way to combine photocatalytic film and constructed wetlands.

## 2. Materials and Methods

### 2.1. Construction and Operation of the Experimental Setup

Consistent with the authors' previous study, the water source for this study was a small, mildly eutrophic lake on the campus of Fuzhou University's Qishan Campus in China. The entire experimental setup consisted of a photocatalytic film front-end treatment and a composite iron–carbon constructed wetland ( $\text{PF}\&\text{W}_{\text{IC}}$ ). The  $\text{W}_{\text{IC}}$  consisted of wetlands with two flow regimes—vertical subsurface flow and horizontal subsurface flow—in sequential order. Both the external structure and internal composition of the wetlands were consistent with those in the previous study. The media layer of the vertical subsurface consisted of spherical iron–carbon (0.5–0.8 cm), gravel (1–1.8 cm), and gravel (2–3 cm) from top to bottom; the media layer of the horizontal subsurface consisted of gravel (1–1.8 cm), ellipsoidal iron–carbon (2–3 cm), and gravel (4–6 cm) from top to bottom. The plants in the wetland were all tumbleweeds. The PF layout was also consistent with that of the previous study, with the PF laid flat on the water surface at the front of the  $\text{W}_{\text{IC}}$ . A performance characterization of the PF was completed in another study [35], which showed that the  $\text{TiO}_2$ - $\text{SiO}_2$ -containing photocatalytic film had obvious light absorption between 250 and 400 nm of UV light. Characteristic absorption occurred at about 315 nm, which indicated that the PF had photocatalytic properties; the PF had highly efficient photocatalytic activity under simulated light conditions, with a photodegradation rate of 89.59% in a Methylene

Blue (MB) solution after 10 h of photoreaction. The design of the entire experimental setup is shown in Figure 1. The water quality conditions of the lake are shown in Table 1.

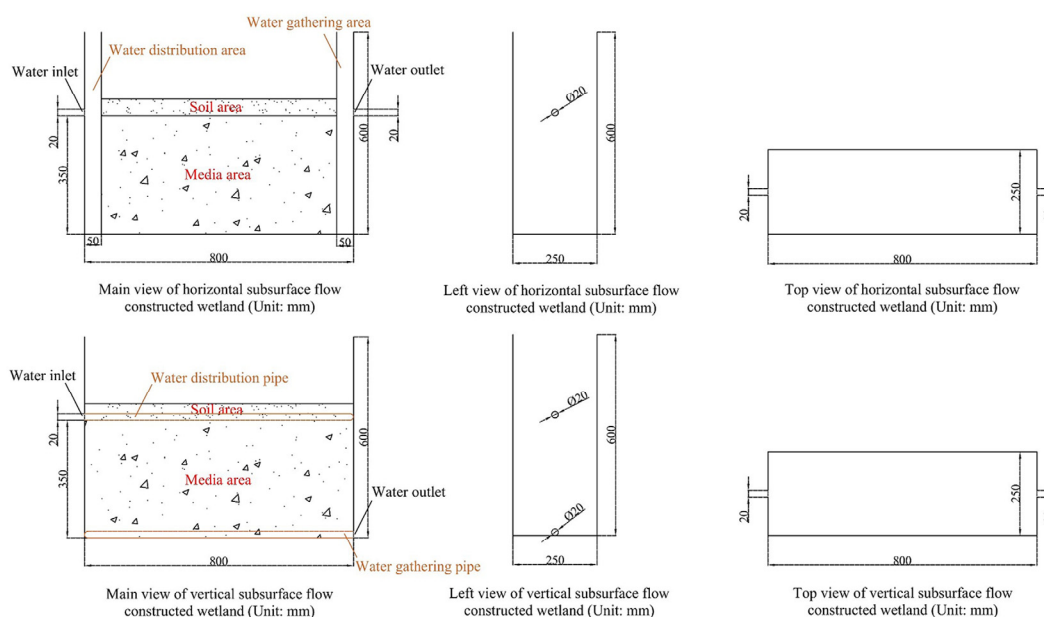


**Figure 1.** Design diagram of the experimental setup.

**Table 1.** Water quality condition of influent water.

Index	Concentration
$\text{NH}_4^+ - \text{N}$ (mg/L)	0.36~0.61
TN (mg/L)	1.76~2.11
TP (mg/L)	0.021~0.034
COD (mg/L)	42.32~55.90
Chlorophyll <i>a</i> ( $\mu\text{g/L}$ )	8.15~13.37
DO (mg/L)	3.70~7.64
pH (non-dimensional)	7.75~8.12

## 2.2. Water Sampling and Analysis

The frequency and duration of the water sample collections were consistent with those in the previous study. The system was divided into four stages (12 h, 24 h, 36 h, and 48 h) according to different hydraulic retention times (HRT) for the experiments. The 12 h stage was operated for 39 days, each of the remaining stages was operated for 21 days, and the samples were taken every three days at sampling intervals ranging from 14:00 to 15:00. After the water samples were collected, they were sent to the laboratory to determine ammonia nitrogen ( $\text{NH}_4^+ - \text{N}$ ), total nitrogen (TN), total phosphorus (TP), and chemical oxygen demand (COD) according to the Standard Methods for the Examination of Water and Wastewater [36], and three parallel tests were performed to eliminate errors. Chlorophyll *a*, DO, and pH were measured at the sampling site using a portable meter, and the probes used in the portable meter were calibrated before each test.

## 2.3. PCR Amplification and Sequencing Library Construction

PCR amplification and sequencing libraries were performed by Majorbio, Inc. (Shanghai, China) using the Illumina PE300/PE250 platform, and PCR amplification of the V3-V4 variable region of the 16S rRNA gene was carried out using the upstream primer 338F (5'-ACTCCTACGGGGAGGCAGCAG-3'), which carries a Barcode sequence, and the downstream primer 806R (5' GGACTACHVGGGTWCTAAT-3'). The PCR reaction system was 4  $\mu\text{L}$  of 5  $\times$  TransStart FastPfu buffer, 2  $\mu\text{L}$  of 2.5 mM dNTPs, 0.8  $\mu\text{L}$  of the upstream primer

(5  $\mu\text{M}$ ), 0.8  $\mu\text{L}$  of the downstream primer (5  $\mu\text{M}$ ). TransStart FastPfu DNA polymerase (TransGen, Beijing, China), 0.4  $\mu\text{L}$ , and template DNA, 10 ng were added to obtain a total of 20  $\mu\text{L}$ . The amplification procedure was as follows: pre-denaturation at 95  $^{\circ}\text{C}$  for 3 min and 27 cycles (denaturation at 95  $^{\circ}\text{C}$  for 30 s, annealing at 55  $^{\circ}\text{C}$  for 30 s, and extension at 72  $^{\circ}\text{C}$  for 30 s), followed by a stable extension at 72  $^{\circ}\text{C}$  for 10 min and storage at 4  $^{\circ}\text{C}$ . (PCR instrument: T100 Thermal Cycler PCR thermocycler (BIO-RAD, Hercules, CA, USA)).

#### 2.4. Statistical and Analysis

SPSS was used to analyze the mean and standard deviation of the experimental data, and Origin and CAD were used to plot the relevant images.

### 3. Results

#### 3.1. Overall Treatment Performance

Section 3.1 describes the effectiveness of PF&W<sub>IC</sub> in removing the pollutants NH<sub>4</sub><sup>+</sup>-N, TN, TP, COD, and chlorophyll *a*, and the along-track changes in pollutant removal. Effluent-0, Effluent-1, Effluent-2, and Effluent-3 in the charts represent effluent locations in the water source, PF, VSSFCW, and HSSFCW, respectively.

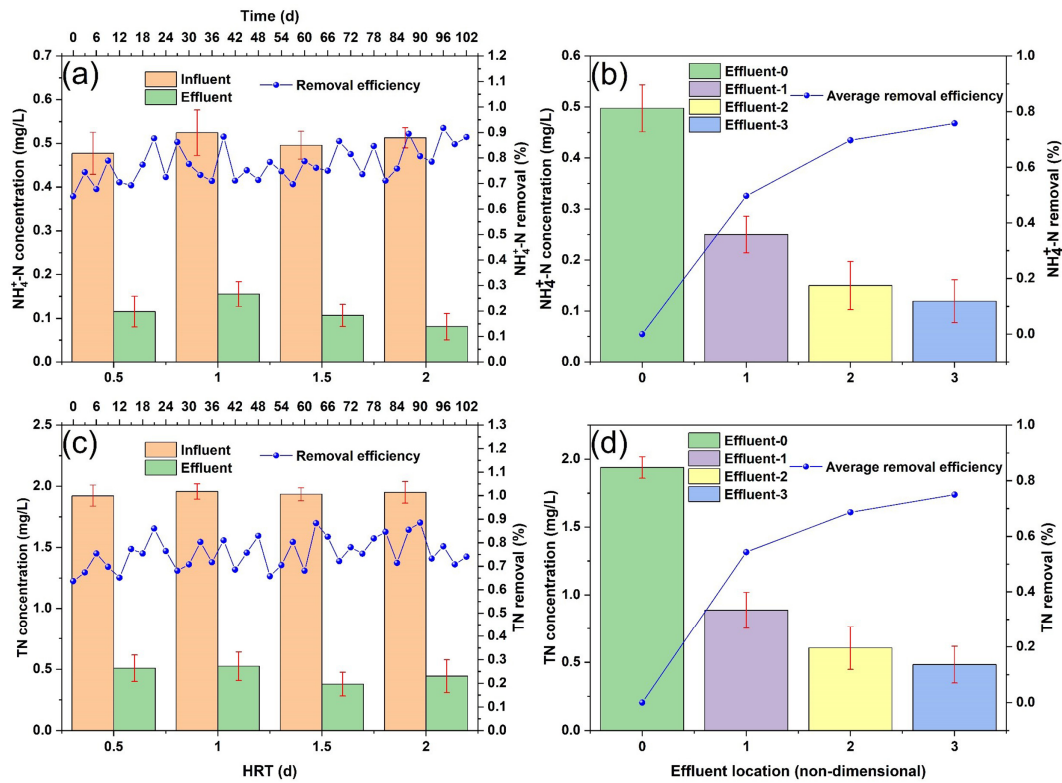
##### 3.1.1. Nitrogen Removal

Figure 2a,c illustrate the effect of PF&W<sub>IC</sub> on the removal of NH<sub>4</sub><sup>+</sup>-N and TN. The overall average removal rates of NH<sub>4</sub><sup>+</sup>-N and TN were 79.1  $\pm$  6.6% and 76.8  $\pm$  6.5%. Compared with our previous study (81.8  $\pm$  7.0% and 79.2  $\pm$  5.6%) [34], the effect of PF&W<sub>IC</sub> on NH<sub>4</sub><sup>+</sup>-N and TN, when PF was used as a front-end treatment, was close to that of W<sub>IC</sub>&PF on TN when PF was used as a back-end treatment. This shows that Fe-C microelectrolysis in the W<sub>IC</sub> plays a dominant role in N removal throughout the treatment process, mainly in that Fe-C microelectrolysis enhances NH<sub>4</sub><sup>+</sup>-N nitrification and the chemical reduction of NO<sub>3</sub><sup>-</sup>-N [37–39].

The removal rates of NH<sub>4</sub><sup>+</sup>-N and TN using PF&W<sub>IC</sub> at different HRTs were 79.5  $\pm$  7.1% and 76.3  $\pm$  6.0% (HRT = 0.5 d); 74.2  $\pm$  3.3% and 73.1  $\pm$  6.1% (HRT = 1.0 d); 78.4  $\pm$  5.5% and 80.4  $\pm$  5.2% (HRT = 1.5 d); and 84.3  $\pm$  5.6% and 77.4  $\pm$  6.5% (HRT = 2.0 d). Previously, Xiaona Ma used iron and carbon (Fe-C) microelectrolysis in a constructed wetland system to denitrify mariculture wastewater, and the removal rate of NH<sub>4</sub><sup>+</sup>-N was 41.5% [40].

Figure 2b,d illustrate NH<sub>4</sub><sup>+</sup>-N and TN removal with PF&W<sub>IC</sub> at different effluent locations. The average removal rates of NH<sub>4</sub><sup>+</sup>-N and TN in Effluent-1, Effluent-2, and Effluent-3 were 50.4  $\pm$  5.9% and 54.1  $\pm$  6.8%; 71.7  $\pm$  9.5% and 70.7  $\pm$  8.0%; and 78.0  $\pm$  8.2% and 76.8  $\pm$  6.5%, respectively. This shows that the water body removes most of the NH<sub>4</sub><sup>+</sup>-N and TN after secondary treatment with PF and VSSFCW, with HSSFCW making a more limited contribution to TN removal. At the same time, the removal rate of PF for NH<sub>4</sub><sup>+</sup>-N and TN was not high, and it is difficult to meet the treatment requirements if only PF is used.

Overall, removing NH<sub>4</sub><sup>+</sup>-N and TN from a water body relies on Fe-C microelectrolysis. PF makes little difference in overall N removal efficiency, whether it is used as a front-end or back-end treatment for the W<sub>IC</sub>. Secondary treatment with PF and VSSFCW can remove most of the TN, but PF should not be used alone for N removal.



**Figure 2.** Nitrogen removal performance of PF&W<sub>IC</sub>. ((a):  $\text{NH}_4^+\text{-N}$  concentration histogram and  $\text{NH}_4^+\text{-N}$  removal efficiency curve at different HRT; (b):  $\text{NH}_4^+\text{-N}$  concentration histogram and  $\text{NH}_4^+\text{-N}$  removal efficiency curve at different effluent location; (c): TN concentration histogram and TN removal efficiency curve at different HRT; (d): TN concentration histogram and TN removal efficiency curve at different effluent location).

### 3.1.2. Phosphorus Removal

Figure 3a illustrates the effect of PF&W<sub>IC</sub> on TP removal. The overall average removal rate of TP was  $77.0 \pm 5.4\%$ . Compared with our previous study ( $80.5 \pm 4.9\%$ ) [34], the effect of PF&W<sub>IC</sub> on TP, when PF was used as a front-end process, was close to the effect of W<sub>IC</sub>&PF on TP when PF was used as a back-end process. This shows that the removal of TP throughout the treatment process is mainly dependent on chemical precipitation.  $\text{Fe}^{2+}$  and  $\text{Fe}^{3+}$  produced by Fe-C microelectrolysis are the key to P removal. When the Fe-C microelectrolysis electrode is under neutral or alkaline conditions,  $\text{Fe}^{2+}$  and  $\text{Fe}^{3+}$  form  $\text{Fe}_3(\text{PO}_4)_2$  and  $\text{FePO}_4$  precipitates with  $\text{PO}_4^{3-}$ , which can remove phosphorus [41,42]. The removal rates of TP using PF&W<sub>IC</sub> at different HRTs were  $77.8 \pm 5.1\%$  (HRT = 0.5 d),  $73.2 \pm 5.8\%$  (HRT = 1.0 d),  $79.8 \pm 4.7\%$  (HRT = 1.5 d), and  $77.4 \pm 3.6\%$  (HRT = 2.0 d). Previously, Cheng Dong used iron-carbon microelectrolysis combined with a constructed wetland to treat wastewater, showing a phosphorus removal efficiency of 76.1% [43].

Figure 3b illustrates the TP removal effect of PF&W<sub>IC</sub> at different effluent locations. The average removal rates of TP were  $46.1 \pm 5.5\%$ ,  $64.2 \pm 6.2\%$ , and  $77.0 \pm 5.4\%$  for Effluent-1, Effluent-2, and Effluent-3, respectively. This shows that the removal of TP with PF is more limited than N removal with PF and that the water body needs to undergo tertiary treatment with PF, VSSFCW, and HSSFCW to remove most of the TP.

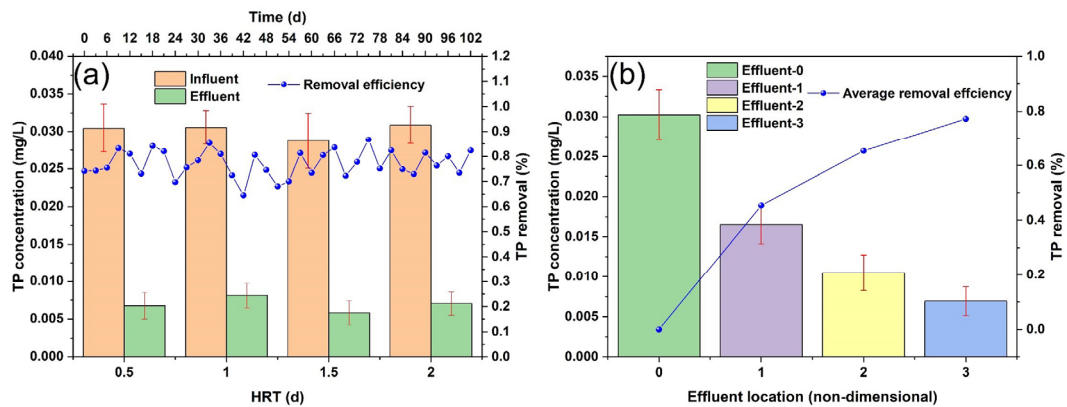
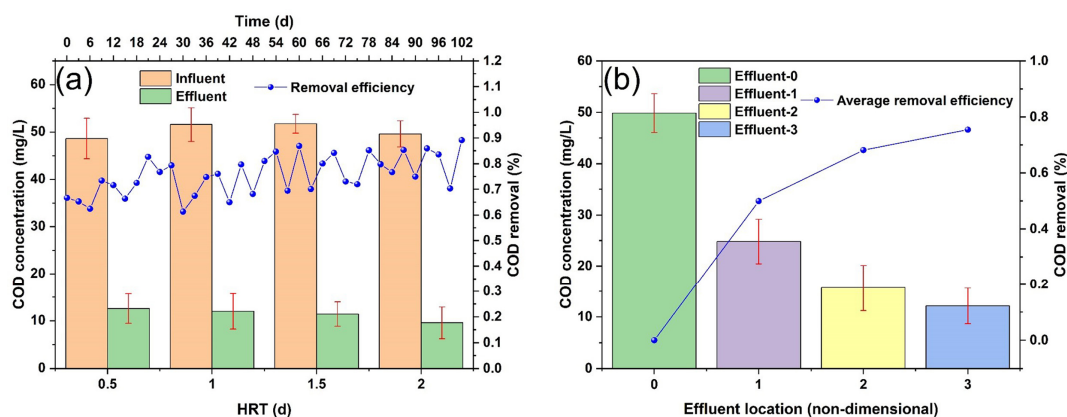


**Figure 3.** Phosphorus removal performance of PF&W<sub>IC</sub>. ((a): TP concentration histogram and TP removal efficiency curve at different HRT; (b): TP concentration histogram and TP removal efficiency curve at different effluent location).

Overall, removing TP mainly depends on the chemical precipitation of Fe<sup>2+</sup> and Fe<sup>3+</sup> produced by Fe-C microelectrolysis. The overall removal efficiency of PF for TP does not differ much whether it is used as a front-end or back-end treatment in the W<sub>IC</sub>. The water body needs to go through a three-stage treatment with PF, VSSFCW, and HSSFCW before most of the TP can be removed. Thus, PF has a very limited ability to remove TP and should not be used alone for P removal.

### 3.1.3. COD Removal

Figure 4a illustrates the effect of PF&W<sub>IC</sub> on COD removal. The overall average removal rate of COD was 77.3 ± 7.2%. Compared with our previous study (80.1 ± 5.9%) [34], when PF was used as a front-end treatment, the effectiveness of PF&W<sub>IC</sub> on COD was close to the effectiveness of W<sub>IC</sub>&PF on COD when PF was used as a back-end treatment. This shows that, during the entire treatment process, COD removal is mainly affected by Fe-C microelectrolysis. The Fe<sup>2+</sup> produced by Fe-C microelectrolysis has high chemical activity that can change the structure and characteristics of organic matter in the water body and accelerate organic matter degradation [30]. The removal rates of COD using PF&W<sub>IC</sub> at different HRTs were 74.0 ± 6.8% (HRT = 0.5 d), 76.4 ± 8.1% (HRT = 1.0 d), 77.8 ± 5.6% (HRT = 1.5 d), and 80.8 ± 6.4% (HRT = 2.0 d). Previously, Xiaoying Zheng combined a constructed wetland and an iron-carbon (Fe-C) system to treat saline wastewater, and the results showed that the COD treatment efficiency was 68.2% [44].



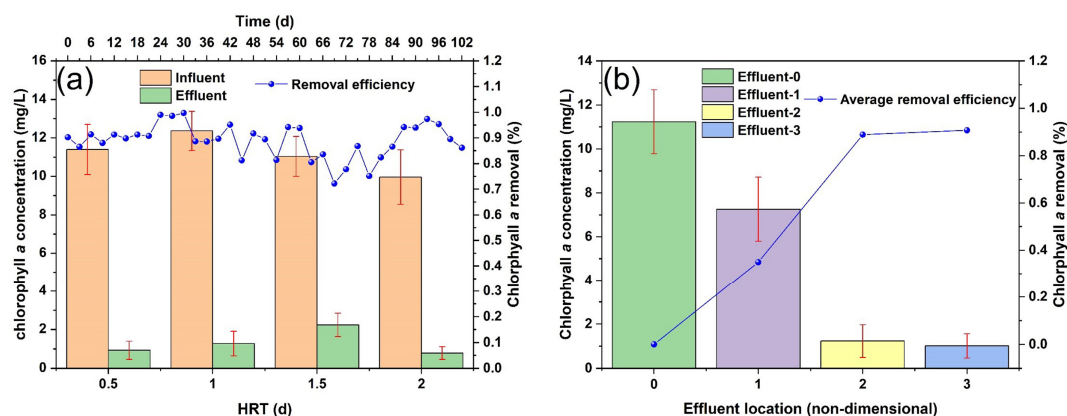
**Figure 4.** COD removal performance of PF&W<sub>IC</sub>. ((a): COD concentration histogram and COD removal efficiency curve at different HRT; (b): COD concentration histogram and COD removal efficiency curve at different effluent location).

Figure 4b illustrates the COD removal effect of PF&W<sub>IC</sub> at different effluent locations. The average removal rates of COD were  $49.7 \pm 11.4\%$ ,  $70.1 \pm 10.7\%$ , and  $77.3 \pm 7.2\%$  for Effluent-1, Effluent-2, and Effluent-3, respectively. This shows that the water body removes most of the COD after secondary treatment with PF and VSSFCW, with HSSFCW making a more limited contribution to COD removal. Similar to the removal ability of PF for TP, the removal ability of PF for COD has difficulty degrading organic matter on its own.

Overall, COD removal was strongly influenced by Fe<sup>2+</sup> produced by Fe-C microelectrolysis. The overall removal of COD with PF was not significantly different whether it was used as a front-end or back-end treatment in the W<sub>IC</sub>. Most of the COD can be removed from the water with a secondary treatment with PF and VSSFCW. PF has a very limited ability to remove COD and should not be used alone to degrade organic matter.

### 3.1.4. Chlorophyll *a* Removal

Figure 5a illustrates the effect of PF&W<sub>IC</sub> on chlorophyll *a* removal. The overall average removal rate of chlorophyll *a* was  $91.7 \pm 5.6\%$ . Compared with our previous study ( $94.0 \pm 4.7\%$ ) [34], the effect of PF&W<sub>IC</sub> on chlorophyll *a*, when PF was used as a front-end treatment, was close to that of W<sub>IC</sub>&PF on chlorophyll *a* when PF was used as a back-end treatment. This shows that removing chlorophyll *a* is mainly achieved through the adsorption and retention effect of the media throughout the entire treatment process, and the rough surface of the iron–carbon media plays a key role in removing chlorophyll *a* [45]. The removal rates of chlorophyll *a* using PF&W<sub>IC</sub> at different HRTs were  $93.55 \pm 4.85\%$  (HRT = 0.5 d),  $89.6 \pm 5.5\%$  (HRT = 1.0 d),  $79.8 \pm 4.7\%$  (HRT = 1.5 d), and  $91.9 \pm 4.1\%$  (HRT = 2.0 d). Figure 5b illustrates the chlorophyll *a* removal effect of PF&W<sub>IC</sub> at different effluent locations. The average removal rates of chlorophyll *a* were  $91.7 \pm 5.6\%$ ,  $88.7 \pm 7.2\%$ , and  $35.9 \pm 13.5\%$  for Effluent-1, Effluent-2, and Effluent-3, respectively. This shows that PF plays a minor role in chlorophyll *a* removal. A previous study showed that PF can provide a carrier for phytoplankton survival [34], thus removing a small fraction of chlorophyll *a*. The water removes most of the chlorophyll *a* after secondary treatment with PF and VSSFCW, with HSSFCW making a more limited contribution to chlorophyll *a* removal.



**Figure 5.** Chlorophyll *a* removal performance of PF&W<sub>IC</sub>. ((a): Chlorophyll *a* concentration histogram and Chlorophyll *a* removal efficiency curve at different HRT; (b): Chlorophyll *a* concentration histogram and Chlorophyll *a* removal efficiency curve at different effluent location).

Overall, chlorophyll *a* was removed mainly via the adsorptive retention of the iron–carbon packing material. The overall removal efficiency of PF for chlorophyll *a* did not differ much whether it was used as a front-end or back-end treatment in the W<sub>IC</sub>. Most of the chlorophyll *a* is removed from the water by a secondary treatment with PF and VSSFCW. PF can provide a vehicle for phytoplankton survival, but it cannot be used alone for chlorophyll *a* removal.

### 3.2. Changes in the Physicochemical Environment

Section 3.2 describes changes in the DO and pH caused by PF&W<sub>IC</sub> and along-track changes in DO and pH. Effluent-0, Effluent-1, Effluent-2, and Effluent-3 in the charts represent effluent locations in the water source, PF, VSSFCW, and HSSFCW, respectively.

#### 3.2.1. Changes in DO

DO is one of the most important indicators of a water body's capacity for self-purification. Changes in DO concentration have a significant effect on NH<sub>4</sub><sup>+</sup>-N nitrification and COD degradation [46,47]. Figure 6a shows that the highest DO concentration in the effluent was achieved at HRT = 2.0 d, while NH<sub>4</sub><sup>+</sup>-N and COD were also optimally removed at HRT = 2.0 d (Sections 3.1.1 and 3.1.3). The DO concentration in the final HSSFCW effluent decreased significantly compared with that of the raw water, and the DO concentrations from the raw water caused by the PF, VSSFCW, and HSSFCW effluents showed successive increasing and decreasing trends (Figure 6b). The subsequent decrease in the DO concentration caused by the VSSFCW and the HSSFCW effluent further weakened nitrification and COD degradation (Sections 3.1.1 and 3.1.3). This reaffirms the good reoxygenation effect of PF, which is consistent with the results of a previous study [34]. The entire PF&W<sub>IC</sub> process leads to a reduced DO concentration compared with that of the water source, which is contrary to the W<sub>IC</sub>&PF results [34]. With the same influent used in our previous study, the DO concentrations in the PF&W<sub>IC</sub> effluent decreased by 41.3%, 35.9%, 46.8%, and 18.4%, while the DO concentrations in the W<sub>IC</sub>&PF effluent increased by 1.5%, 7.7%, 15.0%, and 3.4%.

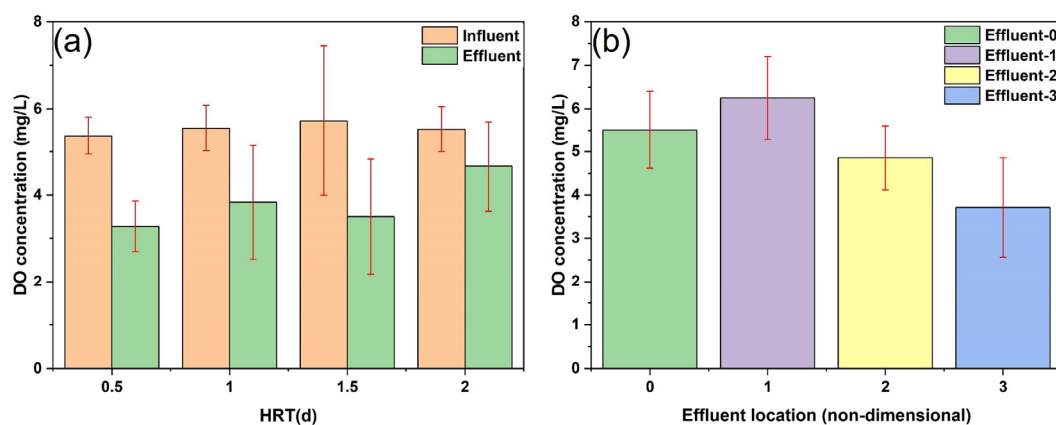


**Figure 6.** Changes in DO in PF&W<sub>IC</sub>. ((a): DO concentration histogram at different HRT; (b): DO concentration histogram at different effluent location).

#### 3.2.2. Changes in pH

Likewise, pH has a significant impact on water quality. The pH of natural water bodies is the most favorable for aquatic organisms when it is between 6 and 9, and the pH of the PF&W<sub>IC</sub> effluent in this study met this requirement (Figure 7b). Changes in pH mainly affect ammonia in the water column; the higher the pH, the more difficult it is for NH<sub>4</sub><sup>+</sup>-N to remain in the water column in an ionized form [48]. In this study, the pH reached a maximum at HRT = 2.0 d (Figure 7a), and the removal rate was highest at HRT = 2.0 d (Section 3.1.1). The pH of the raw water in reaction to the PF, VSSFCW, and HSSFCW effluents showed a gradual increase, which was also related to the effect of Fe-C microelectrolysis (Neutral and alkaline waters) [30]. The pH of the final PF&W<sub>IC</sub> effluent was greater than that of the water source, which is consistent with the W<sub>IC</sub>&PF results [34].

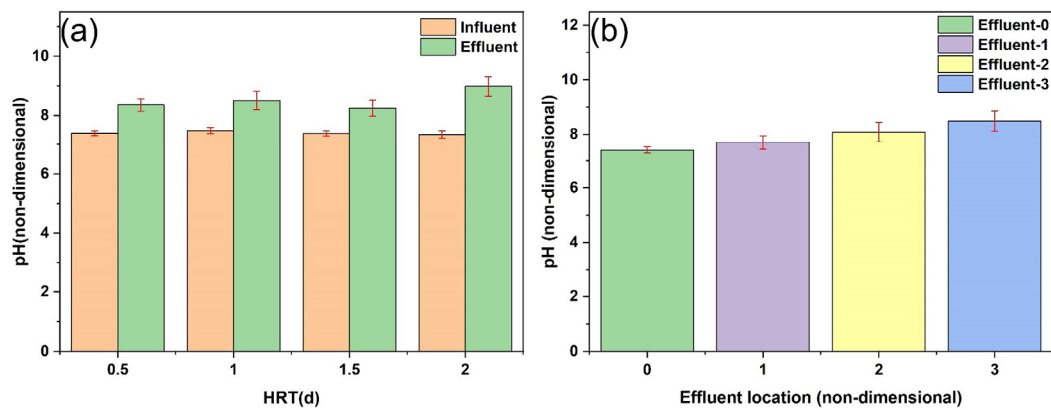


**Figure 7.** Changes in pH in PF&W<sub>IC</sub>. ((a): pH histogram at different HRT; (b): pH histogram at different effluent location).

### 3.3. Microbial Community Analysis

From a phytoplankton point of view, the authors of a previous study found that PF was colonized with a large number of granular *Melosira granulata* via microscopic observation, which greatly increased the growth density of granular *Melosira granulata* in a limited volume [34]. *Melosira granulata* is a *Bacillariophyta* alga, which is a photosynthetic autotrophic organism capable of releasing oxygen through photosynthesis to increase DO concentrations in water bodies [49]. We analyzed bacterial species and their abundance in lake water (LW), photocatalytic film (PF), and lake water treated with PF&W<sub>IC</sub> (LWPF) using the high-throughput sequencing method [50]. Figure 8 shows that the most dominant bacterial types in LW were the hgcl clade (28.6%) and the CL500-29 marine group (12.5%). These are the main genera involved in nitrogen–phosphorus cycling in the pond water; thus, they play an important role in maintaining this balance in ponds [51,52]. Figure 9 shows that the most dominant bacterial species on the PF surface were *Exiguobacterium* (25.0%) and *Enterobacteriaceae* (22.5%). *Exiguobacterium* can use small-molecule carbon sources, such as glucose for anaerobic respiration, and it is capable of degrading small-molecule organic matter in water bodies [53,54]. *Enterobacteriaceae* are well adapted to their environments and can reduce nitrate to nitrite [55], which is then further converted into nitrogen by other denitrifying bacteria (*Massilia*) [53]. Figure 10 shows that the bacterial species and abundance in the lake water after the PF&W<sub>IC</sub> treatment changed significantly, with the most dominant bacterial types in the LWPF being *Cyanobium PCC-6307* (31.2%) and *Enterobacteriaceae* (28.2%). *Cyanobium PCC-6307* is an alga of the phylum Cyanobacteria, which is a photosynthetic autotrophic type of bacteria and has a strong photosynthetic oxygen-releasing capacity [56]. This further explains the reoxygenation of the water body. Furthermore, the percentage of chloroplast in the lake water after the PF&W<sub>IC</sub> treatment reached 11.52%, which was mainly influenced by the root growth of wetland plants [57].

Community analysis pieplot on Genus level :LW

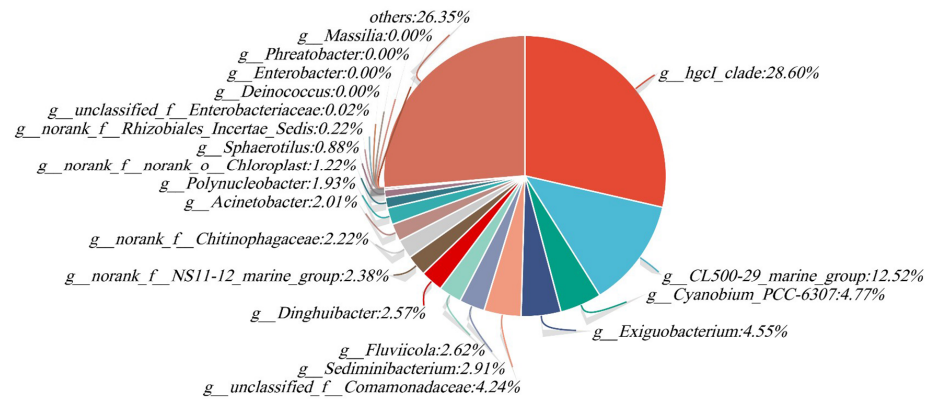


Figure 8. Classification of bacteria in the LW.

Community analysis pieplot on Genus level :PF

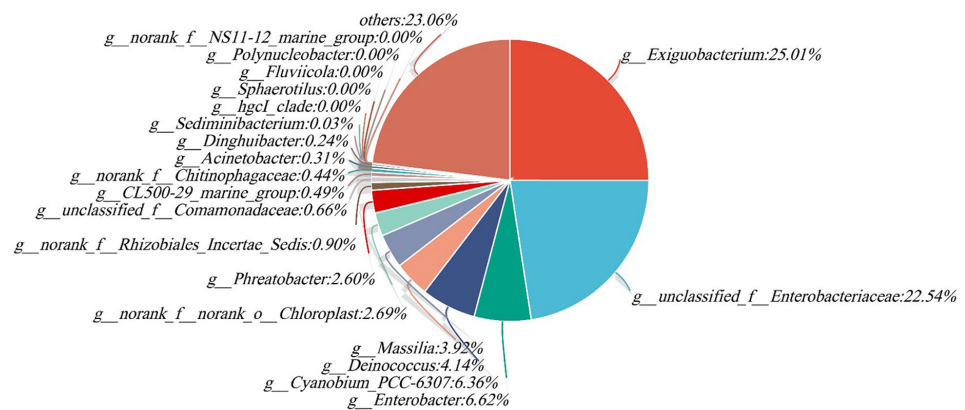


Figure 9. Classification of bacteria in the PF.

Community analysis pieplot on Genus level :LWPF

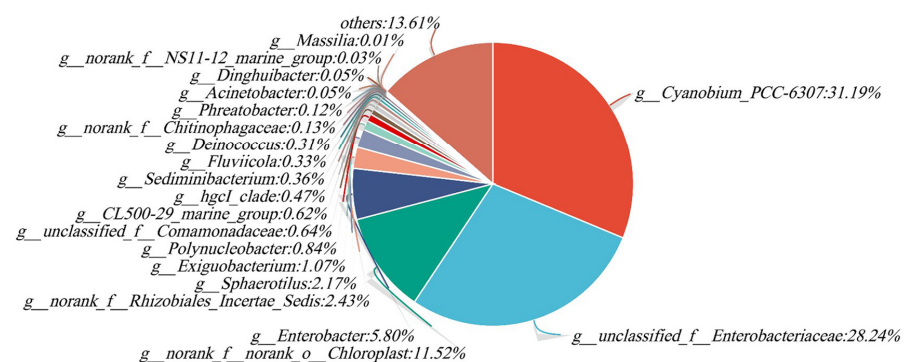


Figure 10. Classification of bacteria in the LWPF.

#### 4. Conclusions

We proposed a treatment process using photocatalytic film as a front-end treatment (PF&W<sub>IC</sub>) for a composite iron-carbon constructed wetland, and it was used to restore a mildly eutrophic water body. The innovation of this study lies in the development of a novel wetland system that integrates a photocatalytic film with iron carbon. This combination significantly influences the variety and quantity of bacteria present in the

lake water. Furthermore, it effectively enhances the dissolved oxygen concentration within the wetland. This is achieved by fostering the proliferation of a substantial number of photosynthetic autotrophic bacteria. We showed that the removal rates of  $\text{NH}_4^+ - \text{N}$ , TN, TP, COD, and chlorophyll *a* using PF&W<sub>IC</sub> were  $79.1 \pm 6.6\%$ ,  $76.8 \pm 6.5\%$ ,  $77.0 \pm 5.4\%$ ,  $77.3 \pm 7.2\%$  and  $91.7 \pm 5.6\%$ , respectively. However, owing to the process's limitations, none of the results derived from using PF alone as a treatment were satisfactory. When PF is combined with VSSFCW for secondary treatments, it can effectively remove most nitrogen, COD, and chlorophyll *a*. However, to remove all phosphorus, it is necessary to go through a tertiary treatment process, which involves the combined application of PF, VSSFCW, and HSSFCW. Therefore, combining PF with other wetland treatment technologies needs to be comprehensively considered in order to achieve optimal water quality improvement. Compared with W<sub>IC</sub>&PF in the authors' previous study, PF&W<sub>IC</sub> was close to W<sub>IC</sub>&PF in removing pollutants, but it was significantly worse than W<sub>IC</sub>&PF in reoxygenating the water body. By using the same influent as in the previous study, the DO concentrations in the PF&W<sub>IC</sub> effluent were decreased by 41.3%, 35.9%, 46.8%, and 18.4%, while the DO concentrations in the W<sub>IC</sub>&PF effluent increased by 1.5%, 7.7%, 15.0%, and 3.4%. The results of our microbial community analysis showed that a large number of photosynthetically autotrophic bacteria were present in the water body treated with PF&W<sub>IC</sub>, and these photosynthetically autotrophic bacteria were one of the main causes of reoxygenation in the water body. There was a significant increase in the population and abundance of bacteria in the PF&W<sub>IC</sub>-treated water. By combining the results of the previous study and the present study, it can be seen that W<sub>IC</sub>&PF is a more reasonable choice for treating eutrophic waters compared with PF&W<sub>IC</sub>, which achieves a similar pollutant removal rate but provides better water body reoxygenation.

**Author Contributions:** Writing—original draft: S.C. and M.Y. Formal analysis: S.C., M.Y. and N.C. Investigation: S.C., M.Y., N.C. and W.P. Data curation: S.C., M.Y. and N.C. Conceptualization: S.C., M.Y. and W.P. Methodology: S.C., M.Y. and W.P. Supervision: W.P. Writing—Review and Editing: W.P. and W.D. Resources: W.P. Funding acquisition: W.P. All authors have read and agreed to the published version of the manuscript.

**Funding:** This research was funded by Research on Water Ecological Restoration Technology Integrated with Photocatalysis Technology of the State Key Laboratory Breeding Base of Photocatalysis of Fuzhou University (83020021).

**Institutional Review Board Statement:** Not applicable.

**Informed Consent Statement:** Not applicable.

**Data Availability Statement:** Experimental data is confidential and not available.

**Conflicts of Interest:** The authors declare that they have no known competing financial interests or personal relationships that could have appeared to influence the work reported in this paper.

## References

1. Fernandez-Fernandez, M.I.; Vega, P.T.M.D.L.; Jaramillo-Morán, M.A.; Garrido, M. Hybrid Constructed Wetland to Improve Organic Matter and Nutrient Removal. *Water* **2020**, *12*, 2023. [[CrossRef](#)]
2. Lu, J.; Guo, Z.; Kang, Y.; Fan, J.; Zhang, J. Recent advances in the enhanced nitrogen removal by oxygen-increasing technology in constructed wetlands. *Ecotox. Environ. Saf.* **2020**, *205*, 111330. [[CrossRef](#)] [[PubMed](#)]
3. Sayer, C.D.; Davidson, T.A.; Jones, J.I. Seasonal dynamics of macrophytes and phytoplankton in shallow lakes: A eutrophication-driven pathway from plants to plankton? *Freshw. Biol.* **2010**, *55*, 500–513. [[CrossRef](#)]
4. Sitoki, L.; Kurmayer, R.; Rott, E. Spatial variation of phytoplankton composition, biovolume, and resulting microcystin concentrations in the Nyanza Gulf (Lake Victoria, Kenya). *Hydrobiologia* **2012**, *691*, 109–122. [[CrossRef](#)] [[PubMed](#)]
5. Yu, C.; Huang, X.; Chen, H.; Godfray, H.C.J.; Wright, J.S.; Hall, J.W.; Gong, P.; Ni, S.; Qiao, S.; Huang, G.; et al. Managing nitrogen to restore water quality in China. *Nature* **2019**, *567*, 516–520. [[CrossRef](#)] [[PubMed](#)]
6. Carstensen, J.; Henriksen, P.; Heiskanen, A.-S. Summer algal blooms in shallow estuaries: Definition, mechanisms, and link to eutrophication. *Limnol. Oceanogr.* **2007**, *52*, 370–384. [[CrossRef](#)]
7. Zhang, C.; Quan, B.; Tang, J.; Cheng, K.; Tang, Y.; Shen, W.; Su, P.; Zhang, C. China's wastewater treatment: Status quo and sustainability perspectives. *J. Water Process Eng.* **2023**, *53*, 103708. [[CrossRef](#)]

8. Lakusic, S. Constructed wetlands for wastewater treatment. *J. Croat. Assoc. Civ. Eng.* **2017**, *69*, 639–652. [[CrossRef](#)]
9. Li, X.; Wu, S.; Yang, C.; Zeng, G. Microalgal and duckweed based constructed wetlands for swine wastewater treatment: A review. *Bioresour. Technol.* **2020**, *318*, 123858. [[CrossRef](#)]
10. Singh, K.K.; Vaishya, R.C. Municipal Wastewater Treatment uses Vertical Flow Followed by Horizontal Flow in a Two-Stage Hybrid-Constructed Wetland Planted with *Calibanus hookeri* and *Canna indica* (Cannaceae). *Water Air Soil Pollut.* **2022**, *233*, 510–521. [[CrossRef](#)]
11. Liang, M.-Y.; Han, Y.-C.; Easa, S.M.; Chu, P.-P.; Wang, Y.-L.; Zhou, X.-Y. New solution to build constructed wetland in cold climatic region. *Sci. Total Environ.* **2020**, *719*, 137124. [[CrossRef](#)]
12. Yi, X.; Lin, D.; Li, J.; Zeng, J.; Wang, D.; Yang, F. Ecological treatment technology for agricultural non-point source pollution in remote rural areas of China. *Environ. Sci. Pollut. Res. Int.* **2021**, *28*, 40075. [[CrossRef](#)] [[PubMed](#)]
13. Lu, M.; Pei, F.F.; Song, X.K.; Guo, Z. Study on the Purification Effects of Constructed Wetland Plants in TP Disposal in Living Wastewater. *Appl. Mech. Mat.* **2012**, *137*, 357–361. [[CrossRef](#)]
14. Shao, L.; Chen, G.Q. Embodied water accounting and renewability assessment for ecological wastewater treatment. *J. Clean. Prod.* **2016**, *112*, 4628–4635. [[CrossRef](#)]
15. Gao, P.; Zhang, C. Study on Phosphorus Removal Pathway in Constructed Wetlands with Thermally Modified Sepiolite. *Sustainability* **2022**, *14*, 12535. [[CrossRef](#)]
16. Lu, S.; Pei, L.; Bai, X. Study on method of domestic wastewater treatment through new-type multi-layer artificial wetland. *Int. J. Hydrogen Energy* **2015**, *40*, 11207. [[CrossRef](#)]
17. Greenway, M. Constructed Wetlands for Water Pollution Control—Processes, Parameters and Performance. *Dev. Chem. Eng. Miner. Process.* **2004**, *12*, 491–504. [[CrossRef](#)]
18. Wu, S.; Kuschik, P.; Brix, H.; Vymazal, J.; Dong, R. Development of constructed wetlands in performance intensifications for wastewater treatment: A nitrogen and organic matter targeted review. *Water Res.* **2014**, *57*, 40–55. [[CrossRef](#)] [[PubMed](#)]
19. Tao, Z.; Jing, Z.; Tao, M.; Kong, Y.; Guan, L.; Jia, Q. A novel filter-type constructed wetland for secondary effluent treatment: Performance and its microbial mechanism. *Bioresour. Technol.* **2023**, *380*, 129075. [[CrossRef](#)]
20. Tao, Z.; Jing, Z.; Tao, M.; Chen, R. Recycled utilization of ryegrass litter in constructed wetland coupled microbial fuel cell for carbon-limited wastewater treatment. *Chemosphere* **2022**, *302*, 134882. [[CrossRef](#)]
21. Roman, M.R.; Brandt, S.B.; Houde, E.D.; Pierson, J.J. Interactive Effects of Hypoxia and Temperature on Coastal Pelagic Zooplankton and Fish. *Front. Mar. Sci.* **2019**, *6*, 139–156. [[CrossRef](#)]
22. Politikos, D.V.; Petasis, G.; Katselis, G. Interpretable machine learning to forecast hypoxia in a lagoon. *Ecol. Inform.* **2021**, *66*, 101480. [[CrossRef](#)]
23. Breitbart, D. Effects of hypoxia, and the balance between hypoxia and enrichment, on coastal fishes and fisheries. *Estuar. Coast.* **2002**, *25*, 767–781. [[CrossRef](#)]
24. Wu, H.; Zhang, J.; Ngo, H.H.; Guo, W.; Hu, Z.; Liang, S.; Fan, J.; Liu, H. A review on the sustainability of constructed wetlands for wastewater treatment: Design and operation. *Bioresour. Technol.* **2015**, *175*, 594–601. [[CrossRef](#)] [[PubMed](#)]
25. Vymazal, J. Do Laboratory Scale Experiments Improve Constructed Wetland Treatment Technology? *Environ. Sci. Technol.* **2018**, *52*, 12956–12957. [[CrossRef](#)] [[PubMed](#)]
26. Lee, C.-G.; Fletcher, T.D.; Sun, G. Nitrogen removal in constructed wetland systems. *Eng. Life Sci.* **2009**, *9*, 11–22. [[CrossRef](#)]
27. Vymazal, J. Removal of nutrients in various types of constructed wetlands. *Sci. Total Environ.* **2007**, *380*, 48–65. [[CrossRef](#)] [[PubMed](#)]
28. Friedrich, J.; Janssen, F.; Aleynik, D.; Bange, H.W.; Boltacheva, N.; Çagatay, M.N.; Dale, A.W.; Etiope, G.; Erdem, Z.; Geraga, M.; et al. Investigating hypoxia in aquatic environments: Diverse approaches to addressing a complex phenomenon. *Biogeosciences* **2014**, *11*, 1215–1259. [[CrossRef](#)]
29. Mallin, M.A.; Johnson, V.L.; Ensign, S.H.; MacPherson, T.A. Factors contributing to hypoxia in rivers, lakes, and streams. *Limnol. Oceanogr.* **2006**, *51 Part 2*, 690–701. [[CrossRef](#)]
30. Li, X.; Jia, Y.; Qin, Y.; Zhou, M.; Sun, J. Iron-carbon microelectrolysis for wastewater remediation: Preparation, performance and interaction mechanisms. *Chemosphere* **2021**, *278*, 130483. [[CrossRef](#)]
31. Jia, L.; Liu, H.; Kong, Q.; Li, M.; Wu, S.; Wu, H. Interactions of high-rate nitrate reduction and heavy metal mitigation in iron-carbon-based constructed wetlands for purifying contaminated groundwater. *Water Res.* **2020**, *169*, 115285. [[CrossRef](#)] [[PubMed](#)]
32. Wang, H.; Li, X.; Zhao, X.; Li, C.; Song, X.; Zhang, P.; Huo, P.; Li, X. A review on heterogeneous photocatalysis for environmental remediation: From semiconductors to modification strategies. *Chin. J. Catal.* **2022**, *43*, 178–214. [[CrossRef](#)]
33. Jabbar, Z.H.; Graimed, B.H.; Ammar, S.H.; Sabit, D.A.; Najim, A.A.; Radeef, A.Y.; Taher, A.G. The latest progress in the design and application of semiconductor photocatalysis systems for degradation of environmental pollutants in wastewater: Mechanism insight and theoretical calculations. *Mater. Sci. Semicon. Process.* **2024**, *173*, 108153. [[CrossRef](#)]
34. Ye, M.; Pan, W.; Dai, W. Composite iron-carbon constructed wetland combined with photocatalytic film to restore eutrophic water body and the hydraulic performance of constructed wetland. *J. Water Process Eng.* **2023**, *53*, 103590. [[CrossRef](#)]
35. Cui, X. Study on the Application of Photocatalytic Synergistic Microalgae in the Treatment of Aquaculture Wastewater. Master's Thesis, Fuzhou University, Fuzhou City, China, 2020. [[CrossRef](#)]

36. Eaton, A.D.; Clesceri, L.S.; Rice, E.W.; Greenberg, A.E. *Standard Methods for the Examination of Water and Wastewater*, 21st ed.; APHA: Washington, DC, USA, 2005.
37. Pu, J.; Feng, C.; Liu, Y.; Li, R.; Kong, Z.; Chen, N.; Tong, S.; Hao, C.; Liu, Y. Pyrite-based autotrophic denitrification for remediation of nitrate contaminated groundwater. *Bioresour. Technol.* **2014**, *173*, 117–123. [[CrossRef](#)] [[PubMed](#)]
38. Deng, S.; Li, D.; Yang, X.; Zhu, S.; Xing, W. Advanced low carbon-to-nitrogen ratio wastewater treatment by electrochemical and biological coupling process. *Environ. Sci. Pollut. Res.* **2016**, *23*, 5361–5373. [[CrossRef](#)] [[PubMed](#)]
39. Ma, Y.; Dai, W.; Zheng, P.; Zheng, X.; He, S.; Zhao, M. Iron scraps enhance simultaneous nitrogen and phosphorus removal in subsurface flow constructed wetlands. *J. Hazard. Mater.* **2020**, *395*, 122612. [[CrossRef](#)] [[PubMed](#)]
40. Ma, X.; Li, X.; Li, J.; Ren, J.; Chi, L.; Cheng, X. Iron-carbon could enhance nitrogen removal in Sesuvium portulacastrum constructed wetlands for treating mariculture effluents. *Bioresour. Technol.* **2021**, *325*, 124602. [[CrossRef](#)] [[PubMed](#)]
41. Xing, C.; Shi, J.; Cui, F.; Shen, J.; Li, H. Fe(2+)/H<sub>2</sub>O<sub>2</sub>-Strengite method with the enhanced settlement for phosphorus removal and recovery from pharmaceutical effluents. *Chemosphere* **2021**, *277*, 130343. [[CrossRef](#)]
42. Leite, S.T.; do Nascimento, F.H.; Masini, J.C. Fe(III)-polyhydroxy cations supported onto K10 montmorillonite for removal of phosphate from waters. *Heliyon* **2020**, *6*, e03868. [[CrossRef](#)]
43. Dong, C.; Li, M.; Zhuang, L.-L.; Zhang, J.; Shen, Y.; Li, X. The Improvement of Pollutant Removal in the Ferric-Carbon Micro-Electrolysis Constructed Wetland by Partial Aeration. *Water* **2020**, *12*, 389. [[CrossRef](#)]
44. Zheng, X.; Jin, M.; Zhou, X.; Chen, W.; Lu, D.; Zhang, Y.; Shao, X. Enhanced removal mechanism of iron carbon micro-electrolysis constructed wetland on C, N, and P in salty permitted effluent of wastewater treatment plant. *Sci. Total Environ.* **2019**, *649*, 21–30. [[CrossRef](#)] [[PubMed](#)]
45. Ahn, Y.; Kwak, S.-Y. Functional mesoporous silica with controlled pore size for selective adsorption of free fatty acid and chlorophyll. *Micropor. Mesopor. Mater.* **2020**, *306*, 110410. [[CrossRef](#)]
46. Hocaoglu, S.M.; Insel, G.; Cokgor, E.U.; Orhon, D. Effect of low dissolved oxygen on simultaneous nitrification and denitrification in a membrane bioreactor treating black water. *Bioresour. Technol.* **2011**, *102*, 4333–4340. [[CrossRef](#)]
47. Shavisi, Y.; Sharifnia, S.; Zendezhaban, M.; Mirghavami, M.L.; Kakehazar, S. Application of solar light for degradation of ammonia in petrochemical wastewater by a floating TiO<sub>2</sub>/LECA photocatalyst. *J. Ind. Eng. Chem.* **2014**, *20*, 2806–2813. [[CrossRef](#)]
48. Fan, J.; Wang, W.; Zhang, B.; Guo, Y.; Ngo, H.H.; Guo, W.; Zhang, J.; Wu, H. Nitrogen removal in intermittently aerated vertical flow constructed wetlands: Impact of influent COD/N ratios. *Bioresour. Technol.* **2013**, *143*, 461–466. [[CrossRef](#)] [[PubMed](#)]
49. Bettencourt, J.H.; Rossi, V.; Renault, L.; Haynes, P.; Morel, Y.; Garçon, V. Effects of upwelling duration and phytoplankton growth regime on dissolved-oxygen levels in an idealized Iberian Peninsula upwelling system. *Nonlinear Process. Geophys.* **2020**, *27*, 277–294. [[CrossRef](#)]
50. Song, Q.; Sun, Z.; Chang, Y.; Zhang, W.; Lv, Y.; Wang, J.; Sun, F.; Ma, Y.; Li, Y.; Wang, F.; et al. Efficient degradation of polyacrylate containing wastewater by combined anaerobic-aerobic fluidized bed bioreactors. *Bioresour. Technol.* **2021**, *332*, 125108. [[CrossRef](#)]
51. Zhou, S.; Sun, Y.; Zhang, Y.; Huang, T.; Zhou, Z.; Li, Y.; Li, Z. Pollutant removal performance and microbial enhancement mechanism by water-lifting and aeration technology in a drinking water reservoir ecosystem. *Sci. Total Environ.* **2020**, *709*, 135848. [[CrossRef](#)]
52. Chao, J.; Li, J.; Kong, M.; Shao, K.; Tang, X. Bacterioplankton diversity and potential health risks in volcanic lakes: A study from Arxan Geopark, China. *Environ. Pollut.* **2024**, *342*, 123058. [[CrossRef](#)]
53. Zhang, L.; Zhong, M.; Li, X.; Lu, W.; Li, J. River bacterial community structure and co-occurrence patterns under the influence of different domestic sewage types. *J. Environ. Manag.* **2020**, *266*, 110590. [[CrossRef](#)] [[PubMed](#)]
54. Mohan Kulshreshtha, N.; Kumar, R.; Begum, Z.; Shivaji, S.; Kumar, A. *Exiguobacterium alkaliphilum* sp. nov. isolated from alkaline wastewater drained sludge of a beverage factory. *Int. J. Syst. Evol. Microbiol.* **2013**, *63 Pt 12*, 4374–4379. [[CrossRef](#)] [[PubMed](#)]
55. Zharikova, N.V.; Markusheva, T.V.; Galkin, E.G.; Korobov, V.V.; Zhurenko, E.Y.; Sitdikova, L.R.; Kolganova, T.V.; Kuznetsov, B.B.; Turova, T.P. *Raoultella planticola*, a new strain degrading 2,4,5-trichlorophenoxyacetic acid. *Appl. Biochem. Microbiol.* **2006**, *42*, 258–262. [[CrossRef](#)]
56. Liu, Q.; Zhang, H.; Chang, F.; Xie, P.; Zhang, Y.; Wu, H.; Zhang, X.; Peng, W.; Liu, F. eDNA revealed in situ microbial community changes in response to *Trapa japonica* in Lake Qionghai and Lake Erhai, southwestern China. *Chemosphere* **2022**, *288*, 132605. [[CrossRef](#)]
57. Li, J.-Y.; Yang, C.; Tian, Y.-Y.; Liu, J.-X. Regulation of Chloroplast Development and Function at Adverse Temperatures in Plants. *Plant Cell Physiol.* **2022**, *63*, 580–591. [[CrossRef](#)] [[PubMed](#)]

**Disclaimer/Publisher's Note:** The statements, opinions and data contained in all publications are solely those of the individual author(s) and contributor(s) and not of MDPI and/or the editor(s). MDPI and/or the editor(s) disclaim responsibility for any injury to people or property resulting from any ideas, methods, instructions or products referred to in the content.